

Heat capacity of α -GaN: Isotope effects

R. K. Kremer,* M. Cardona, and E. Schmitt

Max-Planck-Institut für Festkörperforschung, Heisenbergstrasse 1, D-70569 Stuttgart, Germany

J. Blumm

NETZSCH-Gerätebau GmbH, D-95100 Selb, Germany

S. K. Estreicher and M. Sanati

Physics Department, Texas Tech University, Lubbock, Texas 79409-1051, USA

M. Bockowski, I. Grzegory, and T. Suski

Institute of High Pressure Physics, Polish Academy of Sciences, ulica Sokolowska, 01-142 Warszawa, Poland

A. Jezowski

Institute of Low Temperature and Structure Research, Polish Academy of Sciences, ulica Okolna, 50-422 Wrocław, Poland

(Received 21 March 2005; published 16 August 2005)

Until recently, the heat capacity of GaN had only been measured for polycrystalline powder samples. Semiempirical as well as first-principles calculations have appeared within the past few years. We present in this article measurements of the heat capacity of hexagonal single crystals of GaN in the 20–1400 K temperature range. We find that our data deviate significantly from the literature values for polycrystalline materials. The dependence of the heat capacity on the isotopic mass has also been investigated recently for monatomic crystals such as diamond, silicon, and germanium. Multiatomic crystals are expected to exhibit a different dependence of these heat capacities on the masses of each of the isotopes present. These effects have not been investigated in the past to our knowledge. We also present first-principles calculations of the dependence of the heat capacities of GaN, as a canonical binary material, on each of the Ga and N masses. We show that they are indeed different, as expected from the fact that the Ga mass affects mainly the acoustic, that of N the optic phonons. It is hoped that these calculations will encourage experimental measurements of the dependence of the heat capacity on isotopic masses in binary and more complex semiconductors.

DOI: [10.1103/PhysRevB.72.075209](https://doi.org/10.1103/PhysRevB.72.075209)

PACS number(s): 65.40.–b, 63.20.Dj, 65.40.Ba

I. INTRODUCTION

The investigation of the heat capacity of crystals is an old topic of condensed matter physics with which illustrious names were early associated.^{1–3} Knowledge of the heat capacity of a substance not only provides essential insight into its vibrational properties but is also mandatory for many applications.

Two famous limiting cases are correctly predicted by the standard elastic continuum theory.³ At high temperatures, the constant-volume heat capacity C_v tends to the Petit and Dulong limit, e.g., ~ 49.9 J/mol K in binary materials such as GaN.⁴ At sufficiently low temperatures, C_v is proportional to T^3 .³ At intermediate temperatures, however, the temperature dependence of C_v is governed by the details of vibrations of the atoms and for a long time could only be determined from experiments. In recent years, the temperature dependence of the specific heat of many systems has been calculated in the harmonic approximation. The calculations ranged from semiempirical, based on inelastic neutron scattering or x-ray data, to first principles, based on total energy calculations.

For example, for GaN, a very topical semiconductor these days, the temperature dependence of the specific heat capacity has been calculated, in the harmonic approximation, on the basis of either experimental or first-principles phonon frequencies. The phonon frequencies were obtained semiem-

pirically, from inelastic neutron⁵ or x-ray scattering data⁶ or from first principles, based on electronic calculations of total energies.⁷

In the past 15 years a variety of semiconductor crystals with different isotopic compositions have been grown.⁸ Using these crystals, the effects of the isotopic mass on the phonon spectra,⁹ in particular the related anharmonic effects, have been investigated. Of considerable interest has also been the dependence of the electronic spectra on isotopic mass, which is effected by the electron-phonon interaction.¹⁰ The influence of the isotopic masses on thermomechanical properties, including the thermal conductivity,^{11–14} the thermal expansion,¹⁵ and the specific heat,^{16–18} has also been investigated. Monatomic materials such as diamond, Si, and Ge have only one average isotopic mass that can be varied (effects of fluctuations in the isotopic mass will not be discussed here). GaP and GaAs are binary compounds but their anions have only one stable isotope; hence only the effects of varying the cation isotope mass can be investigated [even so, very interesting effects have been seen in the Raman phonons of GaP (see Ref. 19)].

GaN is an ideal material to investigate isotope effects: Ga possesses two stable isotopes, (⁶⁹Ga and ⁷¹Ga), whereas N has also two such isotopes, ¹⁴N and ¹⁵N. An investigation of the electronic energy gap of GaN and its dependence on the isotopic mass of N was published recently.²⁰ Corresponding

measurements in which the isotopic mass of gallium is varied were, at that time, not possible because of the lack of suitable isotopically modified samples: they are being performed now.

Isotopically modified samples of GaN large enough to measure the dependence of the heat capacity on the masses of Ga and N are still not available. In this paper we present first-principles results concerning this problem, in the hope that they will encourage crystal growth with isotopically pure Ga and N. Our theoretical results are displayed, in the Debye manner, as C_v/T^3 , for the four possible isotope combinations, compared with the calculations for GaN with the natural isotopic abundances. The maximum in C_v/T^3 found at about 40 K increases when any of the isotopic masses is increased, this effect being larger for gallium than for nitrogen. The effect of the latter becomes larger than that of the former at higher temperatures. We also present the calculated logarithmic derivative of C_v/T^3 vs each of the two masses: the effect of the mass of nitrogen is shown to be displaced to higher temperatures with respect to that of the mass of gallium. This can be qualitatively attributed to the fact that the gallium mass affects mainly the acoustic phonons of GaN whereas that of N affects mainly the optical phonons. The temperature dependence of the logarithmic derivatives of C_v/T^3 is compared with the results obtained for monatomic crystals, in which only one mass can be varied.

Due to the difficulties involved in growing large enough single crystals, the experimental results available thus far for GaN have been obtained for polycrystalline powder samples only.^{22–25} In this article, we present measurements of the heat capacity in the range 20–1400 K of single crystals of GaN grown by the high-pressure, high-temperature technique. Our heat capacity data are in good agreement with the results of the first-principles calculations. However, particularly above room temperature, the heat capacities previously obtained on powder samples, and commonly quoted in the literature as standard values, deviate significantly from our data and first-principles theory. We therefore suggest that the standard values for the heat capacity of GaN should be reconsidered and replaced.

II. EXPERIMENT

GaN single crystals were grown by a self-seeding process at pressures of nitrogen of about 1.5 GPa and temperatures of 1800 K from a nitrogen solution in a droplet of gallium.^{26–28} The crystals used in this experiment were of up to 5 mm² lateral size and thickness of 40–300 μm. They have a good crystallographic quality (x-ray diffraction rocking curves of 30–100 arc sec). They were highly conductive ($n > 5 \times 10^{19}$ cm⁻³) due to unintentionally introduced oxygen donors but showed a very low concentration of dislocations, which did not exceed 10² cm⁻². After removing the crystals from the high-pressure growth chamber they were etched in aqua regia which can result in traces of Ga₂O₃ on the etched surfaces of the crystal plates.

The heat capacities in the temperature range 15 < T < 400 K were measured using a commercial physical property measurements system calorimeter (Quantum Design,

6325 Lusk Boulevard, San Diego, CA) employing the relaxation method. To thermally anchor the crystals to the sample holder platform, a minute amount of Apiezon-N grease was used. The total heat capacity of the platform and grease was determined in a separate run and subtracted from the measurements for the GaN crystals. The heat capacities in the temperature range 300 < T < 750 K were measured with a Perkin-Elmer Pyris 1 differential scanning calorimeter (DSC) (Perkin-Elmer, 45 William Street, Wellesley, MA 02481-4078) in a Pt crucible. A total of three independent runs were merged and fitted with a polynomial. The deviation of the experimental points from this polynomial was always less than ±1.5%. The maximum observed difference between data points for the different runs was ≈2%. In the temperature range 350 < T < 1400 K we used a Netzsch 404C Pegasus DSC calorimeter (NETZSCH-Gerätebau GmbH, Wittelsbacher Strasse 42, D-95100 Selb, Germany) with the sample contained in a Pt crucible equipped with alumina liners. For the DSC measurements several crystals were combined to obtain samples with masses between 20 and 60 mg. During the measurement the DSC calorimeters were flushed with N₂ gas. The calibration of the DSC calorimeters was done with a sapphire crystal.

III. FIRST-PRINCIPLES CALCULATIONS

The theoretical results described below were obtained from self-consistent, first-principles calculations based on local density-functional theory with the SIESTA code,^{29,30} as described in Ref. 31. The exchange-correlation potential of Ceperley and Alder,³² parametrized by Perdew and Zunger,³³ was used. Norm-conserving pseudopotentials in the Kleinman-Bylander form³⁴ were used to remove the core regions from the calculations. The basis sets for the valence states were linear combinations of numerical atomic orbitals (double ζ with a set of d orbitals for Ga). The host crystal was represented by a (wurtzite) Ga₃₆N₃₆ periodic supercell. The calculated lattice constants and bulk modulus were found to be $a=3.200$ Å, $c/a=1.629$, and $B=211$ GPa, respectively, which compare well with the literature values³⁵ (3.189 Å, 1.607, and 202 GPa, respectively).

The matrix elements of the (harmonic) dynamical matrices were extracted at $T=0$ K from the derivatives of the density matrix relative to nuclear coordinates using the perturbative approach developed by Baroni *et al.*³⁶ and Gonze *et al.*³⁷ and implemented into SIESTA by Pruneda *et al.*³⁸ The dynamical matrix was then evaluated at 120 q points along high-symmetry directions of the Brillouin zone. This procedure generated some 2.6×10^4 normal mode frequencies. The phonon density of states (PDOS) shown in Fig. 1 was obtained by smoothing the normal-mode frequencies with Gaussians with a width of 1 cm⁻¹.

In the harmonic approximation, the Helmholtz free energy is given by^{39,40}

$$F_{\text{vib}}(T) = k_B T \int_0^\infty \ln[\sinh(\hbar\omega/2k_B T)] g(\omega) d\omega \quad (1)$$

where k_B is the Boltzmann constant. Here, the PDOS $g(\omega)$ is normalized so that $\int g(\omega) d\omega = 3N$, where N is the number of

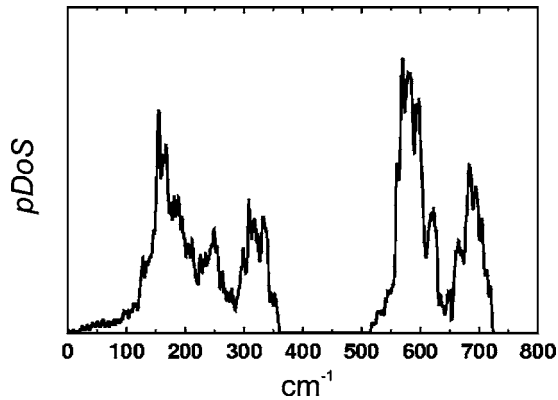


FIG. 1. Calculated phonon density of states of GaN taken from Ref. 7. The band below 400 cm^{-1} corresponds basically to Ga vibrations (except in the acoustic region below $\approx 100 \text{ cm}^{-1}$ where both atoms vibrate). The optical band, above 500 cm^{-1} , corresponds to nitrogen vibrations.

atoms. Note that $F_{\text{vib}}(T=0)$ is the total zero-point energy. Once F_{vib} is calculated, the vibrational entropy and specific heat at constant volume are given by

$$S_{\text{vib}} = - \left(\frac{\partial F_{\text{vib}}}{\partial T} \right)_v, \quad C_v = -T \left(\frac{\partial^2 F_{\text{vib}}}{\partial T^2} \right)_v. \quad (2)$$

In Fig. 2, we display C_v/T^3 calculated in the 20–60 K range for six isotopic compositions, including natural Ga (natural nitrogen can be assumed to be pure ^{14}N for our purposes). This figure clearly illustrates that the effect of changing the mass of Ga is considerably larger than that of changing the mass of N in the temperature region under consideration. This is because the vibrations of nitrogen take place at much higher frequency than those of Ga (see Fig. 1). Figure 3 shows the logarithmic derivatives of C_v/T^3 vs the masses of either the Ga or the N atoms, as well as vs temperature calculated from the data of Fig. 2. This plot was particularly useful for monatomic crystals because it could be related to either the measured^{16,17} or calculated temperature dependence of specific heat by the equation¹⁸

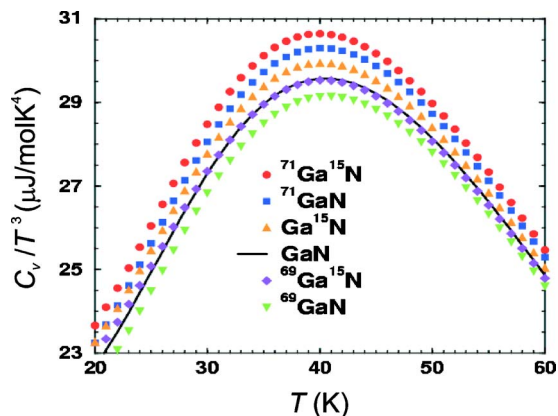


FIG. 2. (Color online) Calculated C_v/T^3 for GaN with various isotope compositions.

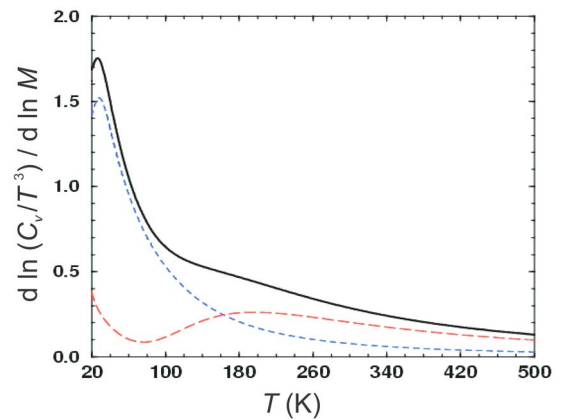


FIG. 3. (Color online) Right-hand side of Eq. (3) (solid black line) compared to the left-hand side $d \ln(C_v/T^3)/d \ln M$ with $M = M_{\text{Ga}}$ [short-dash line (blue)] and $M = M_{\text{N}}$ [long-dashed line (red)]. Note that the sum of the two dashed lines is roughly equal to the solid line.

$$\frac{d \ln(C_v/T^3)}{d \ln M} = \frac{1}{2} \left(\frac{d \ln(C_v/T^3)}{d \ln T} + 3 \right). \quad (3)$$

We have also plotted in Fig. 3 a curve obtained with Eq. (3) using the data of Fig. 4. In comparing this plot with the calculated 0 K values of both derivatives, we realize that the results of Eq. (3) correspond roughly to the sum of the two separate derivatives. This is understood by considering that in the monatomic case the masses of both atoms in the unit cell are varied when taking the mass derivative, whereas in the binary case we vary only one at a time. In the limit ($T \rightarrow 0$) Eq. (3) yields a derivative equal to $3/2$. The logarithmic derivatives vs mass in the binary case (e.g., GaN) are then given by²¹

$$\frac{d \ln C_v}{d \ln M_{\text{Ga}}} = \frac{3}{2} \frac{M_{\text{Ga}}}{M_{\text{Ga}} + M_{\text{N}}} = 1.25, \quad (4)$$

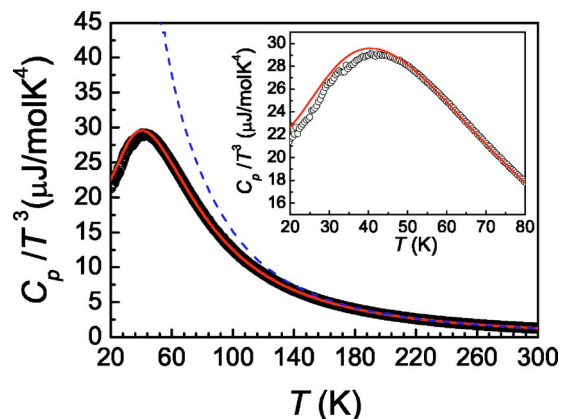


FIG. 4. (Color online) Low-temperature experimental molar heat capacity C_p/T^3 of wurtzite GaN (circles). The solid (red) line represents the results of the first-principles calculations for C_v/T^3 ($C_v \approx C_p$). The dashed (blue) line represents the data obtained by Koshchenko *et al.* on a polycrystalline sample (Ref. 22). The inset shows the region of the Debye maximum in an enlarged scale. Because of the finite size of the unit cell, the first-principles calculations are not meaningful below $\sim 20 \text{ K}$.

$$\frac{d \ln C_v}{d \ln M_N} = \frac{3}{2} \frac{M_N}{2M_{\text{Ga}} + M_N} = 0.25. \quad (5)$$

The sum of both derivatives in Eqs. (4) and (5) equals 3/2, as predicted for a monatomic crystal. This trend can already be seen in the derivatives shown in Fig. 3 for 20 K. In this figure, the gallium derivative remains larger than the nitrogen derivative up to about 160 K. At this temperature the contribution of the gallium to C_v has already flattened out considerably, while tending to the Petit and Dulong limit, whereas that of nitrogen has begun to rise up and takes over.

Notice that below 80 K the derivative vs M_N increases down to 20 K, the lowest temperature we could reliably reach in our calculations. This can be attributed to a dominant contribution of long-wavelength acoustic phonons which include vibrations of Ga as well as of N (the appropriate effective mass is $M_{\text{Ga}} + M_N$). The maximum in the M_N derivative seen in Fig. 3 at ~ 220 K corresponds to that found for the M_{Ga} derivative at 30 K. It signals the rising contribution of the nitrogen-related acoustic phonons.

IV. EXPERIMENTAL RESULTS AND DISCUSSION

Figure 4 displays our low-temperature molar heat capacity data for crystalline GaN as a Debye plot (C_p/T^3 vs T), together with the results of the first-principles calculations in the temperature range $20 < T < 300$ K. For these temperatures, thermal expansion contributions to the heat capacity are negligible, and to a very good approximation, $C_p \approx C_v$ (see the discussion below).

The agreement of our results with the first-principles calculations is very good; small deviations ($< 2.5\%$) are visible below the maximum at ~ 40 K. The magnitude of the Debye maximum is well reproduced in the experimental data; T_{max} is shifted by 1.5 K to higher temperatures from the value predicted by the calculations. For comparison we also show the data by Koshchenko *et al.*²² obtained from measurements of a polycrystalline sample. Below ~ 200 K Koshchenko *et al.*'s data, taken so far as the standard values for the low-temperature heat capacity of GaN, deviate significantly from the first-principles results and the present experimental data. They completely fail to reproduce the maximum at ~ 40 K, which is due to deviations from a T^3 power-law behavior at low temperatures. We presume that impurities may be the reason for this failure. Above 150 K, Koshchenko *et al.*'s results agree fairly well with our data and the first-principles results. The heat capacities determined by Leitner *et al.* for temperatures $200 < T < 1300$ K (not shown in Fig. 4) consistently lie above our data. Up to 300 K the difference does not exceed 2%.

We discuss next our heat capacity results in the the temperature range $300 < T < 1400$ K where the difference between constant-volume and constant-pressure specific heats becomes increasingly important. The constant-volume and constant-pressure specific heats are related by⁴¹

$$C_p(T) = C_v(T) + E(T)T, \quad (6)$$

with

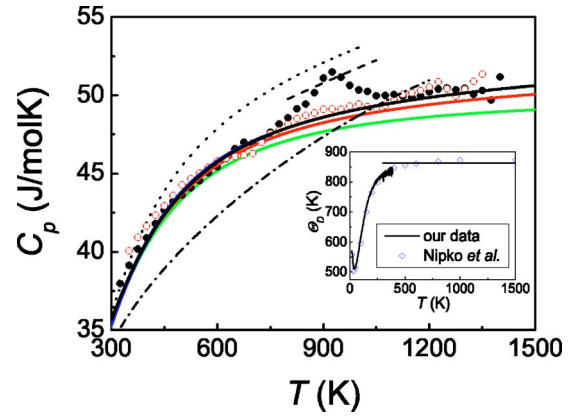


FIG. 5. (Color online) The experimental heat capacities C_p of wurtzite GaN crystals compared with theoretical results. The upper solid (black) line represents the best fit of Eq. (8) to all our data (except the anomaly around 600 K; see text). The lowest solid (green) line represents the first-principles C_v data by Sanati *et al.* (Ref. 7). The middle solid (red) line shows C_p as calculated according to Eqs. (6) and (7) using the literature values for the bulk modulus and the molar volume and the expansion coefficients for the volume thermal expansion $\alpha_v(T)$ as given in the text. The high-temperature data collected with the Netzsch calorimeter (\bullet , \circ) show an anomaly at ~ 900 K, most likely due to the sublimation of traces of Ga_2O (see text). A concomitant small weight loss has been observed in a TGA trace in the corresponding temperature region. The dotted (black), the dashed (black), and the dash-dotted lines show literature data by Leitner *et al.* (Ref. 23), Itagaki *et al.* (Ref. 24), and Chen *et al.* (Ref. 25), respectively. The inset displays the Debye temperatures corresponding to our data according to the Debye law ($20 < T < 400$ K), in comparison with Nipko *et al.*'s results (Ref. 5). To fit the high-temperature data with Eq. (8) a temperature-independent Debye temperature Θ_∞ , indicated by the horizontal bar, has been assumed.

$$E(T) = \alpha_v^2(T)BV_{\text{mol}}, \quad (7)$$

where $\alpha_v(T)$ is the temperature-dependent volume coefficient of thermal expansion, B the bulk modulus, and V_{mol} the molar volume at $T=0$ K. The linear thermal expansion coefficients $\alpha_a(T)$ and $\alpha_c(T)$ have been measured by x-ray diffraction over a wide temperature range ($100 < T < 1500$ K) by Wang and Reeber.⁴² The volume thermal expansion coefficient $\alpha_v(T) = 2\alpha_a(T) + \alpha_c(T)$ amounts to $12.29 \times 10^{-6} \text{ K}^{-1}$ at 300 K and it increases to $15.57 \times 10^{-6} \text{ K}^{-1}$ at 1500 K. Above 200 K the overall temperature dependence of the volume thermal expansion coefficient can be well described by $\alpha_v(T) = [15.59(4) \times 10^{-6} \text{ K}^{-1}][1 - 0.25(1) \times 10^5 \text{ K}^2]/T^2 + [0.50(8) \times 10^9 \text{ K}^4]/T^4$. The overall agreement of this fit with the experimental results is better than $\pm 1\%$.

Figure 5 shows our measured molar heat capacities C_p of crystalline GaN in comparison with the data available in the literature for polycrystalline GaN. The data by Leitner *et al.*²³ and Yamaguchi *et al.*,²⁴ obtained on powder samples and commonly quoted as standard values for the specific heat of GaN at high temperatures, and in particular the data by Chen *et al.*,²⁵ deviate considerably from our results. Above 800 K, our data taken on a pristine sample reveal a broad

hump centered at about 900 K. This anomaly is no longer seen in a subsequent second run carried out on the same sample (see the discussion below). Above 1100 K, the results of both runs agree again within experimental error.

The agreement of our high-temperature heat capacity data with $C_p = C_v + E(T)/T$, with C_v obtained from first principles by Sanati and Estreicher,⁷ is within the expectations for such calculations. To calculate the thermal expansion contribution $E(T)$ according to Eq. (7), the bulk modulus $B = 202.4$ GPa (Ref. 35), the molar volume $V_{\text{mol}} = 13.76 \times 10^{-6}$ m³ and the polynomial fit of the temperature-dependent $\alpha_v(T)$ described in detail above were used.

The solid (black) line in Fig. 5 was obtained by least-squares fitting all our data (for $T \geq 300$ K, excluding the anomaly around 900 K seen in the first run) simultaneously to a power-series expansion of the Debye integral, including terms proportional to $1/T^2$ and $1/T^4$ as well as a term CT to account for the thermal expansion. For simplicity we have assumed a temperature-independent Debye temperature Θ_∞ ,⁴³

$$C_p(T) = 2 \times 3R \left(1 - \frac{1}{20} \frac{\Theta_\infty^2}{T^2} + \frac{1}{560} \frac{\Theta_\infty^4}{T^4} \right) + CT, \quad (8)$$

with R being the gas constant.

Our measured molar heat capacity C_p in the temperature range $300 < T < 1400$ K can be best described with $\Theta_\infty = 863(3)$ K. This Debye temperature correlates very well with the $\Theta_D(T)$ obtained from the measurements around room temperature (~ 840 K) and is consistent with $\Theta_D(T)$ calculated by Nipko *et al.*⁵ from inelastic neutron scattering data (see inset in Fig. 5).

The fit with Eq. (8) gives $C = 1.03 \pm 0.01$ mJ/mol K², somewhat larger than the value of ~ 0.7 mJ/mol K² expected

using the thermal expansion coefficient for $T \rightarrow \infty$ given above.

There is an anomaly centered at ~ 900 K, but starting already at ~ 700 K, in the heat capacity data collected in the first run up to 1400 K. This feature was no longer seen in a subsequent run carried out on the identical sample. Additionally, we detected a small weight loss starting at ~ 600 K which finally amounts to $\sim 0.05\%$ at 1400 K. The heat capacity anomaly and the weight loss indicate sublimation, most likely of the Ga suboxide species Ga₂O. Sublimation of Ga₂O in high vacuum has been found to commence at 500 °C.^{44,45} Since the DSC measurements were carried out in N₂ atmosphere, Ga₂O could result from a reduction of adherent traces of Ga₂O₃ detected after the freshly grown crystals have been etched with aqua regia (see above).

In summary, we determined the heat capacity of GaN single crystals in the temperature range $20 < T < 1400$ K and found significant deviations from the values given in the literature for polycrystalline material. Good agreement of our experimental data with first-principles calculations is observed over the full temperature range. We make detailed predictions as to how the heat capacity will vary if the isotope masses of Ga and N are changed. We hope that these interesting results will soon be confirmed by measurements on isotopically pure GaN crystals.

ACKNOWLEDGMENTS

We thank G. Siegle for expert experimental assistance and U. Klock for preliminary high-temperature heat capacity measurements (not reported here). The work of S.K.E. was supported in part by a grant from the R. A. Welch Foundation.

*Corresponding author. Email address: R.Kremer@fkf.mpg.de

¹A. Einstein, Ann. Phys. **22**, 180 (1907).

²W. Nernst and A. F. Lindemann, Z. Elektrochem. Angew. Phys. Chem. **17**, 817 (1911).

³P. Debye, Ann. Phys. **39**, 789 (1912).

⁴A. T. Petit and P. L. Dulong, Ann. Chim. Phys. **10**, 395 (1819).

⁵J. C. Nipko, C.-K. Lang, C. M. Balleas, and R. F. Davies, Appl. Phys. Lett. **73**, 34 (1998).

⁶T. Ruf, J. Serrano, M. Cardona, P. Pavone, M. Pabst, M. Krisch, M. D' Astuto, T. Suski, I. Grzegory, and M. Leszczynski, Phys. Rev. Lett. **86**, 906 (2001).

⁷M. Sanati and S. K. Estreicher, J. Phys.: Condens. Matter **16**, L327 (2004).

⁸See, e.g., K. W. Itoh, W. L. Hansen, E. E. Haller, J. W. Farmer, V. I. Ozhogin, A. I. Rudnev, and A. I. Tikhomirov, J. Mater. Res. **8**, 1341 (1993).

⁹F. Widulle, J. Serrano, and M. Cardona, Phys. Rev. B **65**, 075206 (2002).

¹⁰M. Cardona, Solid State Commun. **133**, 3 (2004).

¹¹M. Asen-Palmer, K. Bartkowski, E. Gmelin, M. Cardona, A. P. Zhernov, A. V. Inyushkin, A. Taldenkov, V. I. Ozhogin, K. M.

Itoh, and E. E. Haller, Phys. Rev. B **56**, 9431 (1997).

¹²T. Ruf, R. W. Henn, M. Asen-Palmer, E. Gmelin, M. Cardona, H.-J. Pohl, G. G. Devyatych, and P. G. Sennikov, Solid State Commun. **115**, 243 (2000).

¹³R. K. Kremer, K. Graf, M. Cardona, G. G. Devyatych, A. V. Gusev, A. M. Gibin, A. V. Inyushkin, A. N. Taldenkov, and H.-J. Pohl, Solid State Commun. **131**, 499 (2004).

¹⁴L. Wei, P. K. Kuo, R. L. Thomas, T. R. Anthony, and W. F. Banholzer, Phys. Rev. Lett. **70**, 3764 (1993).

¹⁵P. Pavone and S. Baroni, Solid State Commun. **90**, 295 (1994).

¹⁶M. Cardona, R. K. Kremer, M. Sanati, S. K. Estreicher, and T. R. Anthony, Solid State Commun. **133**, 465 (2005).

¹⁷A. Gibin, G. G. Devyatych, A. V. Gusev, R. K. Kremer, M. Cardona, and H.-J. Pohl, Solid State Commun. **133**, 569 (2005).

¹⁸M. Sanati, S. K. Estreicher, and M. Cardona, Solid State Commun. **131**, 229 (2004).

¹⁹F. Widulle, T. Ruf, A. Göbel, E. Schönherr, and M. Cardona, Phys. Rev. Lett. **82**, 5281 (1999).

²⁰F. J. Manjón, M. Hernandez-Fenollosa, B. Mari, S. Li, C. Poweleit, A. Bell, J. Menendez, and M. Cardona, Eur. Phys. J. B **40**, 453 (2004).

- ²¹These equations follow immediately from the Debye model using chain differentiation. They are exact in the harmonic approximation.
- ²²V. I. Koshchenko, A. F. Demidenko, L. D. Sabanova, V. E. Yachmenev, Yu. M. Gran, and A. F. Radchenko, *Izv. Akad. Nauk SSSR, Neorg. Mater.* **15**, 1686 (1979) [*Inorg. Mater.* **15**, 1329 (1979)]. These data are also tabulated by S. Krukowski, M. Leszynski, and S. Porowski, in *Properties, Processing and Applications of Gallium Nitride and Related Superconductors*, edited by J. H. Edgar, S. Strite, I. Akasaki, H. Amano, and C. Wetzel, EMIS Datareview Series No. 23 (INSPEC, London, 1999), p. 21.
- ²³J. Leitner, A. Strejc, D. Sedmidubský, and K. Ružička, *Thermochim. Acta* **401**, 169 (2003).
- ²⁴K. Itagaki, K. Yamaguchi, and A. Yazawa, *Jpn. Inst. Met.* **53**, 764 (1989); K. Itagaki and K. Yamaguchi, *Thermochim. Acta* **163**, 1 (1990).
- ²⁵Xiao-Long Chen, Yu-Cheng Lan, Jing-Kui Liang, Xiang-Rong Cheng, Yan-Ping Xu, Tao Xu, Pei-Zhi Jiang, and Kun-Quan Lu, *Chin. Phys. Lett.* **16**, 107 (1999).
- ²⁶J. Karpinski, J. Jun, and S. Porowski, *J. Cryst. Growth* **66**, 1 (1984).
- ²⁷I. Grzegory, M. Bockowski, B. Lucznik, M. Wroblewski, S. Krukowski, J. Weyher, G. Nowak, T. Suski, M. Leszczynski, E. Luitwin-Staszewska, and S. Porowski, in *Nitride Semiconductors*, edited by F. A. Ponce, S. P. Den Baars, B. K. Meyer, S. Nakamura, and S. Strite, MRS Symposia Proceedings No. 482 (Materials Research Society, Pittsburgh, 1998), p. 15.
- ²⁸I. Grzegory, *J. Phys.: Condens. Matter* **13**, 6875 (2001).
- ²⁹D. Sánchez-Portal, P. Ordejón, E. Artacho, and J. M. Soler, *Int. J. Quantum Chem.* **65**, 453 (1997).
- ³⁰E. Artacho, D. Sánchez-Portal, P. Ordejón, A. García, and J. M. Soler, *Phys. Status Solidi B* **215**, 809 (1999).
- ³¹S. K. Estreicher, M. Sanati, D. West, and F. Ruymgaart, *Phys. Rev. B* **70**, 125209 (2004).
- ³²D. M. Ceperley and B. J. Alder, *Phys. Rev. Lett.* **45**, 566 (1980).
- ³³J. P. Perdew and A. Zunger, *Phys. Rev. B* **23**, 5048 (1981).
- ³⁴L. Kleinman and D. M. Bylander, *Phys. Rev. Lett.* **48**, 1425 (1982).
- ³⁵T. Tsuchiya, K. Kawamura, O. Ohtaka, H. Fukui, and T. Kikegawa, *Solid State Commun.* **121**, 555 (2002).
- ³⁶S. Baroni, P. Giannozzi, and A. Testa, *Phys. Rev. Lett.* **58**, 1861 (1987).
- ³⁷X. Gonze and C. Lee, *Phys. Rev. B* **55**, 10355 (1997).
- ³⁸J. M. Pruneda, S. K. Estreicher, J. Junquera, J. Ferrer, and P. Ordejón, *Phys. Rev. B* **65**, 075210 (2002).
- ³⁹A. A. Maradudin, E. W. Montroll, G. H. Weiss, and I. P. Ipatova, *Theory of Lattice Dynamics in the Harmonic Approximation* (Academic, New York, 1971).
- ⁴⁰O. Kubaschewski and C. B. Alcock, *Metallurgical Thermochemistry* (Pergamon, Oxford, 1979).
- ⁴¹N. W. Ashcroft and N. D. Mermin, *Solid State Physics* (Saunders, Philadelphia, 1976).
- ⁴²K. Wang and R. R. Reeber, in *Nitride Semiconductors* (Ref. 27), p. 863.
- ⁴³R. C. Tolman, *The Principles of Statistical Mechanics* (Oxford University Press, Oxford, 1938).
- ⁴⁴A. Brukl and G. Ortner, *Z. Anorg. Allg. Chem.* **203**, 23 (1931).
- ⁴⁵W. Klemm and H. U. v. Vogel, *Z. Anorg. Allg. Chem.* **219**, 45 (1934).